Strength of Low-Frequency EEG Phase Entrainment to External Stimuli Is Associated with Fluctuations in the Brain's Internal State

Verónica Mäki-Marttunen, Alexandra Velinov, and [iD]**Sander Nieuwenhuis**

Cognitive Psychology Unit, Faculty of Social Sciences, Leiden University, Leiden, Alaska 2333, The Netherlands

Abstract

The brain attends to environmental rhythms by aligning the phase of internal oscillations. However, the factors underlying fluctuations in the strength of this phase entrainment remain largely unknown. In the present study, we examined whether the strength of low-frequency electroencephalography (EEG) phase entrainment to rhythmic stimulus sequences varied with the pupil size and posterior alpha-band power, thought to reflect the arousal level and excitability of posterior cortical brain areas, respectively. We recorded the pupil size and scalp EEG while participants carried out an intermodal selective attention task, in which they were instructed to attend to a rhythmic sequence of visual or auditory stimuli and ignore the other perceptual modality. As expected, intertrial phase coherence (ITC), a measure of entrainment strength, was larger for the task-relevant than for the task-irrelevant modality. Across the experiment, the pupil size and posterior alpha power were strongly linked with each other. Interestingly, ITC tracked both variables: larger pupil size was associated with a selective increase in entrainment to the task-relevant stimulus sequence, whereas larger posterior alpha power was associated with a decrease in phase entrainment to both the task-relevant and task-irrelevant stimulus sequences. Exploratory analyses showed that a temporal relation between ITC and posterior alpha power emerged in the time periods around pupil maxima and pupil minima. These results indicate that endogenous sources contribute distinctly to the fluctuations of EEG phase entrainment.

Key words: alpha power; arousal; EEG; entrainment; pupil

Significance Statement

Fluctuations in cortical state powerfully shape the perception of external stimuli. Understanding the physiological signatures of cortical state fluctuations is crucial to understand how the brain selectively attends and switches between internal and external content. We studied how two signatures of attentional state, pupil-linked arousal and power in the alpha band, shape the entrainment of brain activity to low-frequency rhythmic stimuli. Our results reveal common and dissociable influences of these signatures at slow time scales. Furthermore, measuring and including the pupil size and posterior alpha power as covariates in statistical models can help increase statistical power in studies focusing on electroencephalography phase entrainment. Our study provides new evidence on a direct influence of cortical state on the perception of rhythmic stimuli.

Introduction

How we perceive the continuous stream of external sensory stimulation is highly modulated by the internal state of the brain (Mathewson et al., 2012), but the interaction between external and internal mechanisms of attention is still poorly understood. Rhythmic stimuli entrain endogenous oscillatory activity in the brain to the temporal

structure of the stimulus sequence (VanRullen et al., 2014; Ten Oever et al., 2017; Zoefel et al., 2018; Bauer et al., 2021). This "neural entrainment" results in the alignment of the high-excitability oscillatory phase with the predicted onset of the rhythmic stimuli (Lakatos et al., 2008; Stefanics et al., 2010) and provides an advantage for the processing of natural stimuli that are inherently rhythmical, such as speech, music, and repetitive motion (Henry and Obleser, 2012; Lakatos et al., 2019). Although phase alignment of oscillations to external rhythms constitutes an important principle of neural dynamics and attention, little is known about the factors that make the strength of phase entrainment fluctuate over time.

Here, we investigated the impact on low-frequency phase entrainment of two physiological measures known to be highly variable across time: pupil-linked arousal and posterior alpha-band power. Attention during tasks requiring sustained performance commonly fluctuates due to variations in the internal state of vigilance or arousal (Unsworth and Robison, 2017). The pupil size has long been used to measure variations in the arousal level in humans (Bradshaw, 1967). Very low or very high levels of vigilance, as characterized by lapses of attention or task-unrelated thoughts, often occur during periods of small and/or large (pretrial) baseline pupil diameter (Unsworth and Robison, 2016; van den Brink et al., 2016; Madore et al., 2020). Whether and how arousal modulates the strength of neural entrainment, which is an externally directed process, is still unknown.

Changes in posterior alpha-band power, as measured with electroencephalography (EEG), are thought to reflect the excitability of posterior cortical brain areas that process external (sensory) input (Romei et al., 2008; Samaha et al., 2017). Increased alpha power is suggested to facilitate internally directed attention rather than attention to external stimuli (Cooper et al., 2003; Klimesch et al., 2007; Benedek et al., 2014). Lapses of attention and task-unrelated thoughts are associated with increases in pretrial posterior alpha power (O'Connell et al., 2009; Compton et al., 2019; Jin et al., 2019; Madore et al., 2020; Groot et al., 2021). Similarly, a study in nonhuman primates found that periods with high alpha power were characterized by attentional lapses and strongly diminished low-frequency entrainment of neuronal oscillations to task-relevant rhythmic stimulus sequences (Lakatos et al., 2016). These results suggest that alpha power is an index of internal state and would be expected to anti-correlate with the strength of entrainment to a task-relevant sequence of stimuli.

Although the baseline pupil size and posterior alpha have both been associated with attentional state, their interrelation may not be straightforward. Alpha power as a measure of inattention, as reviewed above, would be expected to correlate negatively with pupil size. That is, low arousal would be related to distraction and an increase in the "idling" alpha. However, studies on the relationship between pupil size and posterior alpha power at rest or in pretrial periods have found a positive relation and/or an inverted-U relationship (Hong et al., 2014; van Kempen et al., 2019; Ceh et al., 2020; Podvalny et al., 2021; Pfeffer et al., 2022; Waschke et al., 2019). Therefore, these two signals may reflect brain states that are at least partly dissociable, and we expected that they would distinctly influence neural entrainment.

In this study, we aimed to test whether and how low-frequency phase entrainment is susceptible to modulations in internal state, as indexed by pupil-linked arousal and posterior alpha power. We simultaneously recorded the pupil size and scalp EEG to investigate the relationships between pupil-linked arousal, cortical alpha oscillations, and low-frequency phase entrainment during an intermodal attention task. In the task, rhythmic streams of visual and auditory stimuli were concurrently presented. Participants had to detect infrequent targets in the cued modality and ignore the other modality. A small difference in the repetition rate (visual, 1.1 Hz; auditory, 1.4 Hz) allowed us to separately assess entrainment to the task-relevant and task-irrelevant stimulus sequences. We hypothesized that transient changes in the strength of entrainment to the attended modality would be related to fluctuations in the arousal level of the participants. We also expected that internal neural processes signaled by alpha power would modulate the entrainment level. This study brings novel insights into the interrelation between external and internal attentional mechanisms of the brain.

Materials and Methods

Participants. Thirty-seven students recruited at Leiden University took part in the experimental study. One participant was excluded because the recording was interrupted. EEG data from four participants were excluded from analysis due to excessive artifacts (>50% of epochs rejected) in the attend visual condition. One participant was excluded because of low accuracy (hit rate < 0.5) in the attend auditory condition. Five out of the first 15 participants were excluded because they reported an unforeseen visual illusion, where they perceived the afterimage of the green fixation stimulus having a similar color as the magenta targets, probably caused by a complementary afterimage effect (Manzotti, 2017). As a precaution to avoid this illusion, after the first 15 participants, we changed the color stimulus, as reported below. Performance did not differ between either set of stimuli for the participants included in the final study (hit rate, first round, 0.77 ± 0.05; second round, 0.79 ± 0.07; $T = 0.86$; $p = 0.398$; incorrect responses, first round, 32 ± 30; second round, 38 ± 38; $T = 0.41$; $p = 0.685$). The final sample consisted of 26 participants (mean age, 23 years; age range, 18–28 years; 22 females). Study exclusion criteria included any psychiatric disorders and wearing contact lenses. The experimental protocol was reviewed and approved by the ethics committee of Leiden University. Participants signed a consent form prior to participating and received a compensation of 7.5 euros/hour or course credits.

Task and stimuli. Participants performed an intermodal selective attention task (Fig. 1), based on that used by Lakatos et al. (2016) to study phase entrainment in monkeys. Participants were presented with simultaneous streams of visual and
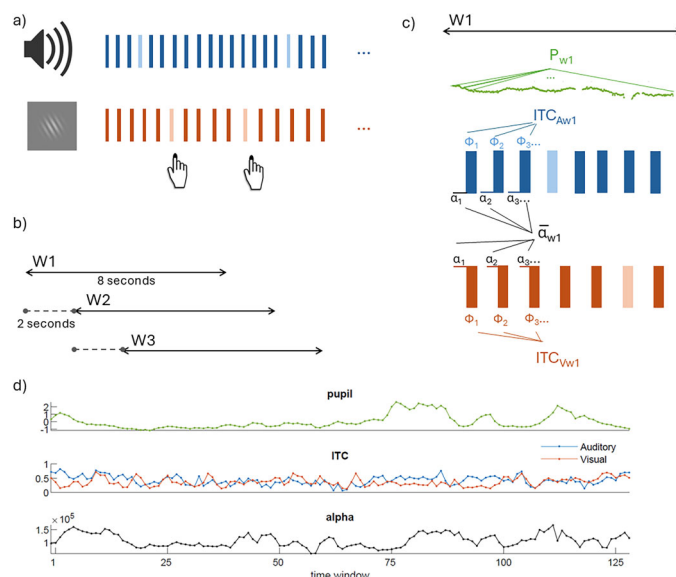
Figure 1. Task and analysis overview. *a*, Multimodal task. Toy example of a sequence of stimuli sequences of the intermodal selective attention task. Rectangles represent stimuli of the auditory modality (tones, represented in blue) and the visual modality (Gabor patches, represented in orange). Auditory and visual stimuli were presented simultaneously at slightly different frequencies (auditory, 1.4 Hz; visual, 1.1 Hz). Participants had to attend to only one modality per block and respond to the target stimuli in that modality (represented in lighter color) with a button press. In this example, the participant responds to the target stimulus in the visual modality—i.e., the visual stimuli were task-relevant. *b*, Illustration of sliding windows approach. The pupil size, ITC, and alpha power were calculated in 8 s sliding windows (W1, W2, W3, etc.) covering the whole block, with 2 s steps. *c*, Illustration of the calculation of ITC over auditory (ITC_A) and visual (ITC_V) stimuli types in one 8 s sliding window. The average pupil size (P, pupil trace in green) was calculated for the entire window. Alpha power for each window was calculated as the average prestimulus alpha power across all stimuli. ITC represented the coherence of phase values at a given frequency across all the trials of the same modality. *d*, A participant's single-block sample data of time courses of the various measures, where each observation represents one time window. These time courses were used to study the relation between pupil, prestimulus alpha power, and ITC.

auditory stimuli and had to respond as quickly as possible to rare target stimuli in the cued modality by pressing the "B" key on a keyboard and to otherwise withhold responding. The response deadline was 1 s after the target onset. The task consisted of 10 blocks, each lasting ~5 min. The participants were prompted at the beginning of each block to attend to the visual stimuli (attend visual condition) or to the auditory stimuli (attend auditory condition) and ignore the other modality. Half of the blocks required the participant to attend to the visual modality and the other half to the auditory modality in a quasirandom order (A1-V1-A2-A3-V2-A4-V3-V4-A5-V5).

In each block, 605 stimuli were presented: 265 visual stimuli and 340 auditory stimuli. In each stream of stimuli, 15% of the stimuli were targets and 85% were standards. The auditory stimuli consisted of short beeps with a 460 Hz pitch for the standards and a 476 Hz pitch for the targets. The visual stimuli consisted of colored RGB Gabor patches (orange standards, RGB 229 133 126; magenta targets, RGB 229 90 172; green fixation point for participants #1-15, RGB 151 199 62; purple fixation point for participants #16-37, RGB 180 137 205) with a 10° orientation and a frequency of 0.1 cycles/pixel, created using an online Gabor-patch generator (https://www.cogsci.nl/gabor-generator). Because changes in luminosity can drive changes in the pupil size, we made sure that the visual stimuli and the interstimuli screens were isoluminant. For this, visual stimuli were made isoluminant with the gray screen background (RGB 167 167 167) using the SHINEcolor toolbox (Dal Ben, 2023). The visual and auditory stimuli were presented at average frequencies of 1.1 and 1.4 Hz, respectively. All stimuli were presented for 50 ms. The fixation point was on the screen in the interval between consecutive visual stimuli, and all visual stimuli subtended a 4° angle on the screen. The average interstimulus interval was 387 ms, with a range from 0 (i.e., auditory and visual stimuli presented simultaneously) to 727 ms. To lower a possible contribution of stimulus-evoked EEG responses to our measure of intertrial phase coherence (ITC), we added to the interstimulus interval some decorrelated jitter, drawn on each stimulus time from the values [−66, −33, 0, 33, 66 ms]. Entrainment occurs at the average (i.e., expected) frequency of presentation of the stimuli and thus is independent of the stimulus presentation itself (Besle et al., 2011).

Procedure. Participants were instructed to sit as still as possible throughout the blocks and to always look at the center of the screen, also in the attend auditory condition. Their chins were positioned in a chin rest, with their eyes at ~73 cm from a monitor with a refresh rate of 60 Hz. For the auditory stimuli, custom in-ear air–tube headphones were used to prevent electrical artifacts in the EEG recordings. Participants first performed two practice blocks, one for each condition, which each lasted 2 min and contained a total of 256 visual and auditory stimuli. After the practice blocks, the eye-tracker was calibrated, and the participants performed the task in a dimly lit room (19.9 lx). The task was controlled using Eprime

3.0 with the appropriate Tobii extensions installed. In between blocks, participants could take breaks and decide when to start the following block. Lighting conditions and screen luminance were kept constant across the whole session. Participants took between 60 and 70 min to complete the experiment.

Time window approach. The purpose of this study was to examine the slow temporal relation between pupil-linked arousal, entrainment, and alpha power. Based on a previous study (Lakatos et al., 2016), we analyzed the pupil and EEG data in sliding time windows. The windows had a length of 8 s and a step size of 2 s, resulting in an overlap of 6 s between consecutive time windows (Fig. 1). The window length and step size were chosen to achieve a balance between the number of stimuli included in each estimate of entrainment (larger number provides a better estimate) and the temporal resolution of our analyses (shorter window length provides higher resolution). Each time window included ~9 visual stimuli and ~11 auditory stimuli.

Given that the paradigm involved the simultaneous presentation of visual and auditory stimuli, each time window contained stimuli in both modalities, but depending on the block, only one of them was task-relevant. For each time window, we obtained the following five measures (Fig. 1): (1) an average pupil size across the entire 8 s window; ITC (a measure of entrainment), which was calculated based on the phase angles at stimulus onset of all (2) visual stimuli and all (3) auditory stimuli of which the onset latency fell within the 8 s window; and average prestimulus alpha power across all (4) visual stimuli and all (5) auditory stimuli of which the onset latency fell within the 8 s window.

Note that in our key analyses, we recoded the visual and auditory stimulus sequences as "task-relevant" and "task-irrelevant," based on the participant's instruction, so that for each 8 s window, we had task-relevant and task-irrelevant ITC and prestimulus alpha power values.

Below, we explain how the pupil size, ITC, and prestimulus alpha power were computed.

Pupillometry.   The pupil diameter of both eyes was recorded using a Tobii Pro X3-120 eye-tracker with a sampling rate of 40 Hz. The calibration was performed at the beginning of the task using a five-point fixation procedure. The Tobii device automatically marked periods when no pupil signal was recorded (e.g., blinks), and the custom code was compiled to save accurate timing data that could then be used to create eye-tracking epochs and segmentations for the behavioral data. Raw pupil data were preprocessed using the PhysioData Toolbox v0.5.0 (Kret and Sjak-Shie, 2019) using the standard pipeline of the Pupil Diameter Analyzer module. One participant was excluded from the pupil analyses due to excessive data loss during preprocessing (>50% of recording). An exponential decay in the pupil size was observed at the beginning of the blocks for most participants. Since the magnitude of such time-on-task effects can obscure the effects of the more subtle trial-by-trial fluctuations in pupil-linked arousal that we were interested in (van den Brink et al., 2016), we fitted an exponential decay curve to the pupil time series using the MATLAB R2018 (MathWorks) functions *fittype* and *fit* and regressed out this component from the pupil data. For the time windows analyses, the continuous pupil signal was cut into 8 s windows (2 s step size) and then averaged across each window. The resulting time series were z-scored separately for each block to make sure that differences in the pupil size reflected local fluctuations in the pupil size instead of global time-on-task effects (Hopstaken et al., 2015).

EEG acquisition and preprocessing. EEG data were recorded using a BioSemi ActiveTwo system with 32 active Ag-AgCl electrodes, at a sampling rate of 512 Hz. The electrodes were arranged according to the international 10–20 system. In addition to the 32 main electrodes, two reference electrodes were positioned on the mastoids, two facial electrodes above and below the left eye, and two electrodes on the temples. Raw EEG data were preprocessed in EEGLAB (Delorme and Makeig 2004). The signal was re-referenced to the mastoids and high-pass filtered (0.5 Hz). Bad channels were removed using *cleanrawdata* function of EEGLAB. The minimal acceptable correlation with nearby channels was set to the default value of 0.8, while the parameter for artifact subspace reconstruction (a method for removing high-amplitude artifacts from EEG data) was set to 10. Missing channels were interpolated from neighboring sites. Then the data were split into attend auditory and attend visual conditions and epoched into 3 s segments centered on the stimulus onset. This epoch length was chosen to avoid edge artifacts in the time–frequency analysis (Besle et al., 2011). Bad epochs were rejected automatically (threshold criteria, 150 µV), and an independent component analysis (infomax algorithm with "extended" option to extract sub-Gaussian sources) was performed to identify and remove noise components manually (e.g., eye artifacts, muscle artifacts). Preprocessing was done using the Neuroscience Gateway (https://www.nsgportal.org, Sivagnanam et al., 2013; Martínez-Cancino et al., 2021).

ITC and prestimulus alpha power. The epoched EEG data were used to calculate measures of phase entrainment and alpha power. We first extracted spectral power and phase dynamics using Morlet wavelet decomposition from 1 to 30 Hz with 30 logarithmically spaced steps. We used a wavelet cycle range of 3–12. This corresponded to a precision, as measured by the spectral full-width at half-maximum, ranging from 0.48 to 5.88 Hz (Cohen, 2019). Entrainment of EEG oscillations to the stimulus rhythms is calculated based on the instantaneous phase values at the frequency and time of presentation of visual and auditory stimuli (Besle et al., 2011; Lakatos et al. 2013). To determine the phase angle at the stimulus onset, we used the 3 s epochs centered on the stimulus onset that were mentioned above (section "EEG acquisition and preprocessing"). Our ITC estimates based on the instantaneous phase at $t = 0$ were not affected by edge-effect

artifacts (i.e., were within the cone of influence). ITC, a measure of the consistency across trials of the phase angle at the time of the stimulus onset (Tallon-Baudry et al., 1996), was calculated with the following formula:

$$ITC(f, t) = \text{abs}(\text{sum}(e^{i*\text{phi}(f,t)})/n),$$

where phi is the phase at frequency f and time point t of a single trial (i.e., stimulus presentation) and n is the number of trials considered. This was done separately for the visual and auditory stimulus streams at the corresponding frequency (1.1 Hz for visual and 1.4 Hz for auditory; Fig. 3a). For these analyses, we averaged data from electrodes displaying the largest ITC for each modality: AF3, AF4, F3, Fz, F4, FC1, and FC2 for auditory stimuli and C3, Cz, C4, CP1, and CP2 for visual stimuli. For the 8 s time window analyses, we computed the ITC across all visual and (separately) auditory stimuli of which the onset latency fell within the 8 s window.

For the analysis of prestimulus alpha power, we extracted for each epoch the data from −500 to 0 msec before the stimulus and applied a fast Fourier transform to extract the power density spectrum (Ergenoglu et al., 2004; Compton et al., 2019). We then calculated the area under the curve for the alpha band (8–13 Hz). Extended Data Figure 3-1 shows the posterior distribution of prestimulus alpha power. We averaged the data of posterior electrodes (P7, P3, Pz, O1, Oz, O2, P4, and P8), obtaining thus one prestimulus alpha value for each stimulus. For the 8 s time window analyses, we computed the average alpha power value across all visual and auditory stimuli of which the onset time fell within the 8 s window. The resulting time series of ITC and alpha power were z-scored separately for each block.

The analyses described above eventually yielded one pupil size value for each 8 s window and two ITC values and two alpha power values for each 8 s window: one for the task-relevant stimulus sequence (visual stimuli in the attend visual condition; auditory stimuli in the attend auditory condition) and one for the task-irrelevant stimulus sequence (visual stimuli in the attend auditory condition; auditory stimuli in the attend visual condition).

Temporal analysis around pupil maxima and minima. We analyzed the variables ITC and prestimulus alpha power in segments of 10 windows around maxima and minima of the pupil timecourse. Because of the overlap between windows, 10 windows corresponded to 26 s. The normalized pupil size timecourse of each participant was thresholded at +1 standard deviation to detect the peaks and −1 standard deviation to detect the troughs. For this, the function *findpeaks* in MATLAB was employed, with a minimum distance between consecutive maxima and consecutive minima of 10 time windows. Then, the normalized ITC and alpha power data were extracted from those windows for further analysis. The cross-correlation between the variables was calculated with the function *xcorr* in MATLAB. To statistically compare cross-correlations between the time-windowed variables around pupil maxima and minima, we used cluster-based permutation testing, with 1,000 iterations and a significance level of $\alpha = 0.01$ for the individual time points and $\alpha = 0.05$ for the significant clusters. All the temporal analyses were performed on the task-relevant modality, and data were collapsed across modalities.

Statistics. The hit rate was defined as the proportion of targets in the cued modality that were detected in time (i.e., button press within 1 s after the target onset). Any response that was not a hit was counted as an incorrect response. Given the overlap between the task-relevant and task-irrelevant stimulus sequences, it was hard to distinguish incorrect responses to standards in the task-relevant modality from responses to the targets of the task-irrelevant modality, and thus we pooled them together as "incorrect responses." Average ITC values were compared with repeated-measure ANOVA with cued modality (attend visual, attend auditory) and stimulus type (visual, auditory) as within-subject factors. To examine the relationships between the pupil size, ITC, prestimulus alpha power, and task performance (hit rate, number of incorrect responses), we aggregated the data of the 8 s time windows in 10 equally populated bins on the basis of one variable and examined the effects of bin (1–10), task relevance (task-relevant vs task-irrelevant stimulus sequence), and stimulus type (visual, auditory) on one of the other variables using a repeated-measure ANOVA. In the analyses of task performance, we included in the model both a linear and quadratic effect of bin. Statistics were performed using MATLAB.

Results

Behavioral results

Participants showed better performance in the attend auditory condition than in the attend visual condition (Fig. 2a). The hit rate was significantly higher ($F_{(1,495)} = 6.78$; $p = 0.009$), whereas the number of incorrect responses did not differ between conditions ($F_{(1,475)} = −0.88$; $p = 0.11$; for statistics, Table 1). We also inspected the relation between the pupil size and task performance. Pupil bin had no linear and quadratic effects on the hit rate ($F_{(1,495)} = 1.79$; $p = 0.18$; $F_{(1,495)} = 2.52$; $p = 0.11$). In contrast, pupil bin had both a linear and a quadratic effect on the number of incorrect responses ($F_{(1,475)} = 22.65$; $p < 0.001$; $F_{(1,475)} = 30.90$; $p < 0.001$). More incorrect responses were made at intermediate levels of the pupil size (Fig. 2a). No significant interactions between pupil size bin and cued modality were observed (hits, $p = 0.64$; incorrect responses, $p = 0.74$).

Prestimulus alpha power showed a qualitatively similar relationship with task performance. Alpha bin had no linear and quadratic effects on the hit rate ($F_{(1,515)} = 0.04$; $p = 0.62$; $F_{(1,515)} = 0.08$; $p = 0.76$). In contrast, alpha bin had both a linear and
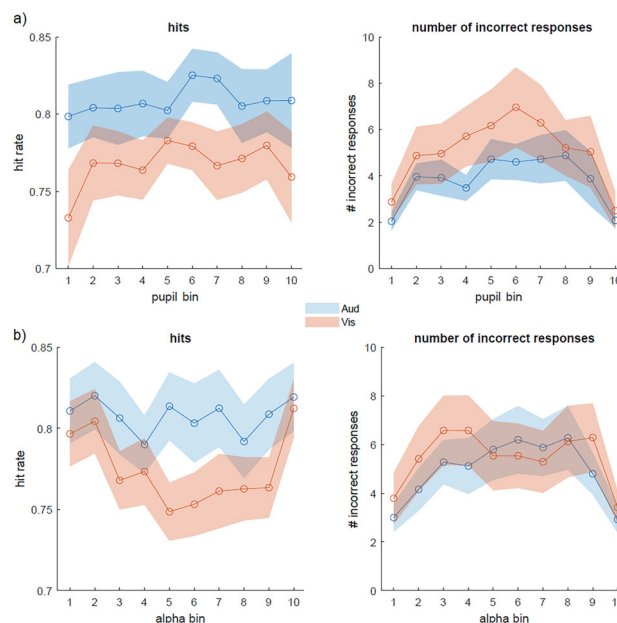
Figure 2. Behavioral results. The hit rate and number of incorrect responses as a function of pupil bin (**a**) and prestimulus alpha bin (**b**). Colors correspond to the different task-relevant modalities (Aud, auditory; Vis, visual).

Table 1. Statistical table

	Data structure	Type of test	p value	Power (95% C.I., min, max)
Figure 2a	Normal distribution	Repeated-measure ANOVA: pupil bin effect	0.92	−0.004, 0.025
	Normal distribution	Repeated-measure ANOVA: bin quadratic effect	0.11	−0.001, 0.0002
	Normal distribution	Repeated-measure ANOVA: Modality effect	0.009	−0.08, −0.011
	Normal distribution	Repeated-measure ANOVA: pupil bin effect	<0.001	1.00, 2.41
	Normal distribution	Repeated-measure ANOVA: bin quadratic effect	<0.001	−0.19, −0.09
	Normal distribution	Repeated-measure ANOVA: modality effect	0.1	−0.28, 2.97
Figure 2b	Normal distribution	Repeated-measure ANOVA: prestimulus alpha bin effect	0.62	−0.01, 0.01
	Normal distribution	Repeated-measure ANOVA: bin quadratic effect	0.76	−0.001, 0.0008
	Normal distribution	Repeated-measure ANOVA: modality effect	0.14	−0.05, 0.008
	Normal distribution	Repeated-measure ANOVA: prestimulus alpha bin effect	<0.001	0.80, 2.39
	Normal distribution	Repeated-measure ANOVA: bin quadratic effect	<0.001	−0.18, −0.07
	Normal distribution	Repeated-measure ANOVA: modality effect	0.05	−0.06, 3.59
Figure 3c	Normal distribution	Repeated-measure ANOVA: task-relevance effect	0.006	−0.05, 0.00
	Normal distribution	Repeated-measure ANOVA: modality effect	<0.001	0.05–0.12
Figure 4a	Normal distribution	Repeated-measure ANOVA: pupil bin effect	0.68	−0.002, 0.003
	Normal distribution	Repeated-measure ANOVA: modality effect	0.844	−0.022, 0.018
	Normal distribution	Repeated-measure ANOVA: attention effect	0.011	−0.046, −0.005
	Normal distribution	Repeated-measure ANOVA: interaction bin * attention	0.005	0.001, 0.007
Figure 4b	Normal distribution	Repeated-measure ANOVA: pupil bin effect	<0.001	0.015, 0.023
	Normal distribution	Repeated-measure ANOVA: modality effect	0.939	−0.010, 0.010
Figure 4c	Normal distribution	Repeated-measures ANOVA: prestimulus alpha bin effect	0.002	−0.007, −0.001
	Normal distribution	Repeated-measure ANOVA: Modality effect	0.058	−0.037, 0.000
	Normal distribution	Repeated-measure ANOVA: attention effect	0.515	−0.012, 0.025
	Normal distribution	Repeated-measure ANOVA: interaction bin * attention	0.445	−0.001, 0.004

a quadratic effect on the number of incorrect responses ($F_{(1,495)} = 15.678$; $p < 0.001$; $F_{(1,495)} = 19.135$; $p < 0.001$). More incorrect responses were made at intermediate levels of prestimulus alpha power (Fig. 2b). No significant interaction between alpha power bin and cued modality was observed (hits, $p = 0.16$; incorrect responses, $p = 0.89$).

Low-frequency phase entrainment to simultaneous trains of auditory and visual stimuli

Figure 3a shows the ITC spectra for the various conditions. The top row shows strong ITC at the frequency corresponding to the task-relevant stimulus sequence (1.4 Hz for attend auditory; 1.1 Hz for attend visual), suggesting entrainment of
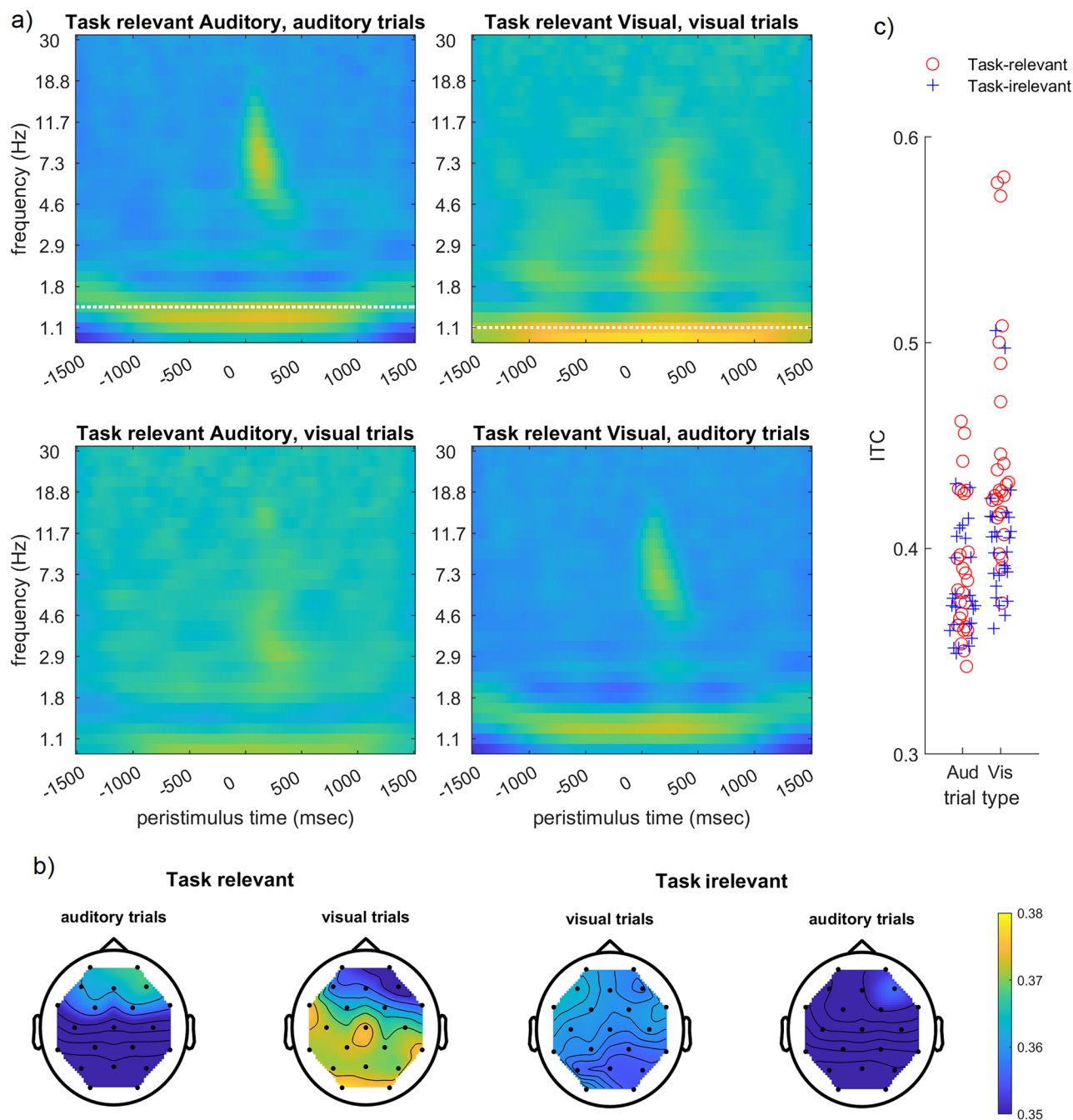
Figure 3. Low-frequency phase entrainment. ***a***, ITC time–frequency spectra, averaged across all electrodes. White horizontal lines indicate the average presentation frequency of auditory (top left) and visual (top right) stimuli. ***b***, Topographies of ITC strength at the peak frequency and the time of the stimulus onset. Topoplots for alpha power are displayed in Extended Data Figure 3-1. ***c***, Average ITC at the driving frequency as a function of task relevance (task-relevant vs task-irrelevant stimulus sequence) and stimulus type.

EEG oscillations to the task-relevant stimulus rhythm. The corresponding ITC topography was frontal for the auditory stimulus sequence and central for the visual stimulus sequence (Fig. 3*b*). The bottom row of Figure 3*a* suggests that EEG oscillations also became entrained to the task-irrelevant stimulus sequences, although significantly less than the task-relevant stimulus sequences (Fig. 3*c*) and with more distributed topographies (Fig. 3*b*). The ITC associated with the task-relevant stimulus sequence was larger in the visual than in the auditory modality ($F_{(1,100)} = 28.67$; $p < 0.001$; Fig. 3*c*), and the difference between entrainment to task-relevant and task-irrelevant stimulus sequences was also larger in the visual modality (interaction task relevance * stimulus type, $F_{(1,100)} = 7.68$; $p = 0.006$; task-relevant vs task-irrelevant, visual, $p < 0.001$; auditory, $p = 0.056$).

Relation between the pupil size, ITC, and prestimulus alpha power

We next inspected the paired associations between the pupil size, ITC, and prestimulus alpha power. ITC did not show a main effect of pupil bin (Fig. 4a; $F_{(1,992)} = 0.16$; $p = 0.68$). However, there was a significant interaction between bin and task relevance ($F_{(1,992)} = 7.74$; $p = 0.005$). Post hoc linear regression analyses showed that with increasing pupil size, the low-frequency oscillations became more entrained to the task-relevant stimulus sequence ($β = 0.005$; $t = 2.22$; $p = 0.026$), while the numerical decrease in entrainment to the task-irrelevant stimulus sequence was nonsignificant ($β = -0.003$; $t = -1.70$; $p = 0.089$).

When looking at prestimulus alpha power, we found a highly significant main effect of pupil bin on alpha power (Fig. 4b; $F_{(1,998)} = 108.27$; $p < 0.001$). Prestimulus alpha power directly increased with pupil size, in line with a previous study (Podvalny et al., 2021). Furthermore, ITC showed a significant main effect of alpha power bin (Fig. 4c; $F_{(1,1032)} = 9.00$; $p = 0.002$), with decreasing ITC as alpha power increased ($β = -0.004$). The interaction with task relevance was not significant ($F_{(1,1032)} = 0.58$; $p = 0.445$).

We did not find any significant main effect of the stimulus type (auditory vs visual) or interaction between the stimulus type and pupil/alpha bin ($p > 0.1$; Extended Data Fig. 4-1), suggesting that the key results reported here generalized across perceptual modalities. Also, our key results could not be explained in terms of enlarged evoked EEG or pupil responses to infrequent target stimuli (Extended Data Fig. 4-2).

Arousal-related modulation of the temporal relation between ITC and alpha power

As an exploratory analysis, we asked whether pupil-linked arousal may modulate the temporal relation between entrainment and alpha power. Specifically, we inspected entrainment and alpha power associated with stimuli of the task-relevant modality in periods centered around pupil maxima and minima (Fig. 5a; Montefusco-Siegmund et al., 2022). Although these maxima and minima roughly correspond to the extreme pupil bins in Figures 2 and 4, a and b, they are partly distinct in that they involve moments in which the derivative of the pupil signal, thought to track distinct changes in cortical state (Reimer et al., 2014; McGinley et al., 2015b), changes sign (e.g., from positive to negative around pupil peaks). We found that pupil maxima were preceded by an increase in entrainment, but this effect was transient and small (Fig. 5b). More interestingly, a large increase in prestimulus alpha was observed prior to pupil maxima and a large decrease prior to pupil minima (Fig. 5c). This indicates that changes in the electrophysiological signatures occurred prior to the changes in pupil-linked arousal. To investigate whether the changes in entrainment and alpha power associated with changes in arousal were linked, we calculated the cross-correlation between these signals around pupil maxima and minima. We found that the temporal relation between entrainment and alpha power was strongly modulated around pupil maxima and minima (Fig. 5d): there was a significant positive correlation between ITC and alpha power in time windows around pupil maxima and a significant negative correlation in time windows around pupil minima. Interestingly, while the positive correlation was transient, the negative correlation lasted for a prolonged time (~18 s). Taken together, the results suggest that changes in ITC and alpha power are temporally related and that this relation is strongly modulated by arousal.

Discussion

The goal of the current study was to unravel how variations in the brain's internal state contribute to fluctuations in neural and behavioral measures of attention at slow timescales. We examined the impact of varying levels of pupil-linked arousal and alpha power on low-frequency phase entrainment. We found that increases in pupil size coincided with stronger entrainment of low-frequency oscillations to the task-relevant stimulus sequence. In contrast, increases in prestimulus
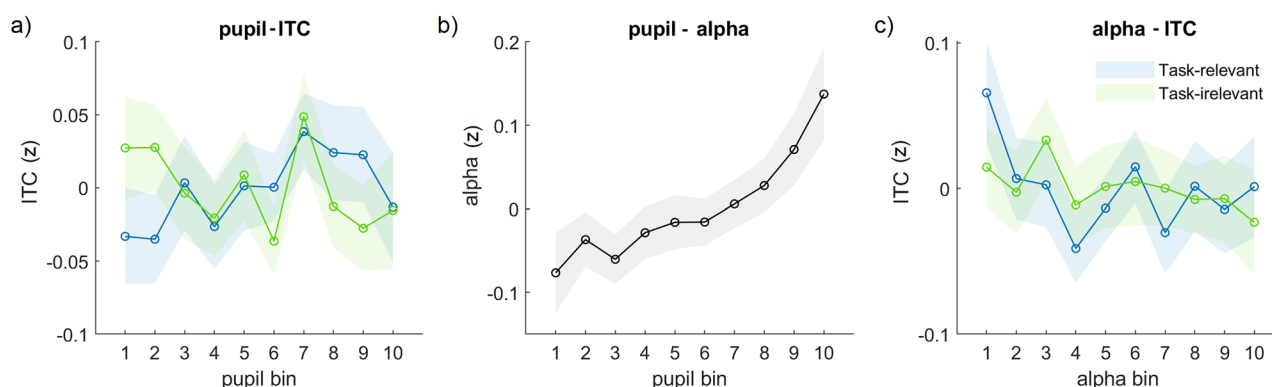

Figure 4. Paired relation between the pupil size, ITC, and alpha power. Relation between (**a**) the pupil size and ITC; (**b**) the pupil size and prestimulus alpha power; and (**c**) prestimulus alpha power and ITC. Different colors correspond to the task-relevant and task-irrelevant modality. Note that the distinction between the task-relevant and task-irrelevant modality is only of interest for ITC. There were no significant main effects and interaction effects of the stimulus type (visual, auditory; Extended Data Fig. 4-1), so we averaged across those levels. The significant effects cannot be explained by the number of targets (Extended Data Fig. 4-2).
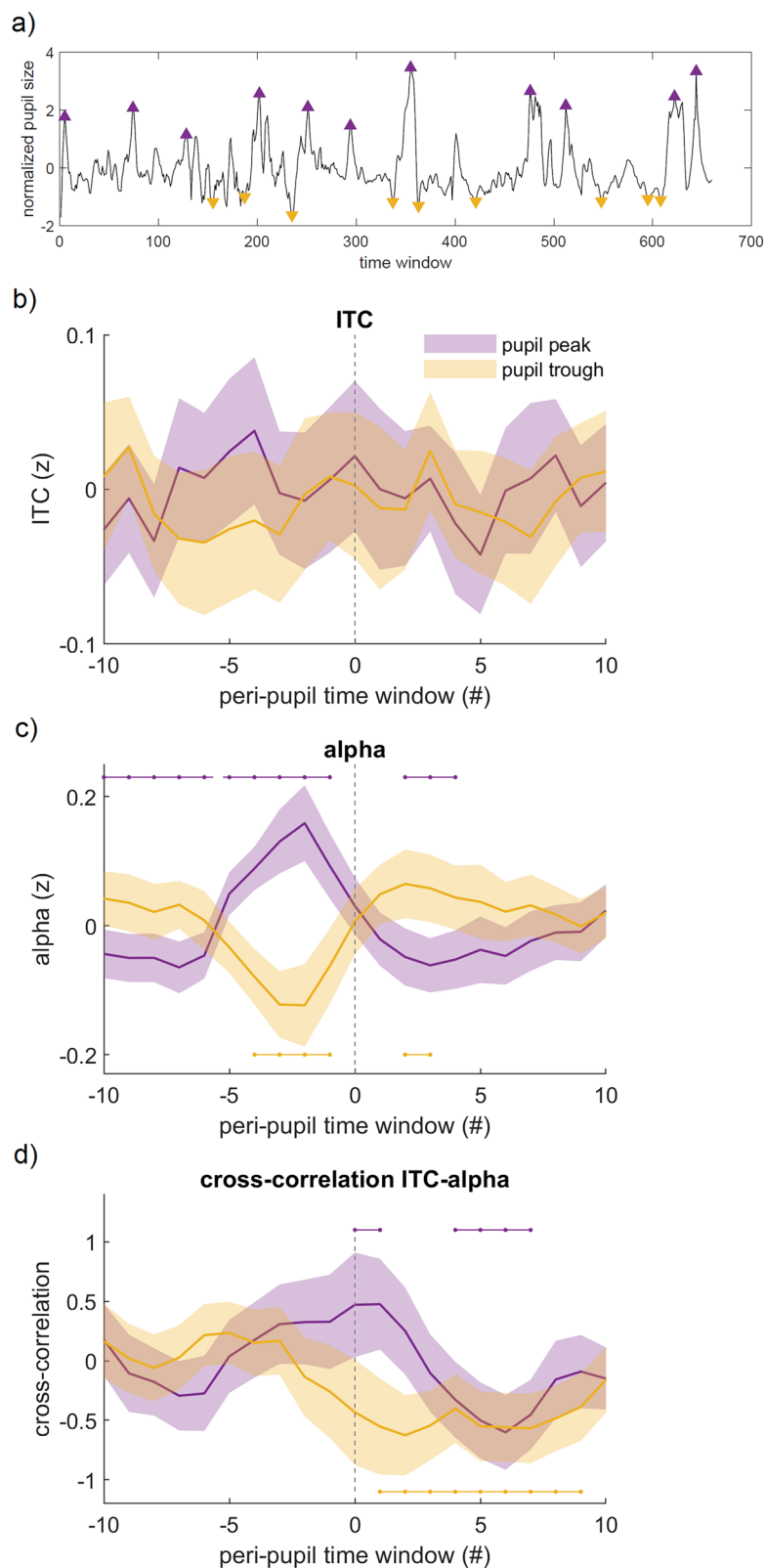
Figure 5. Temporal relation between ITC and prestimulus alpha power around pupil maxima and minima. *a*, Example of one participant's time course of the pupil size and detected maxima and minima marked with yellow and purple triangles, respectively; *b* and *c*, Timecourse of ITC and alpha power, respectively, around pupil peaks and troughs; *d*, cross-correlogram between ITC and alpha power associated with stimuli of the task-relevant modality: around pupil maxima (purple) and around pupil minima (yellow). Negative lags correspond to ITC leading alpha power, while positive lags correspond to alpha power leading ITC. Horizontal lines above and below the time courses indicate significant difference from zero based on permutation testing (*p* < 0.05).

alpha power coincided with a *decrease* in oscillatory phase entrainment to both the task-relevant and task-irrelevant stimulus sequences. Furthermore, we found that alpha power and ITC showed a significant correlation but only in the time windows around pupil maxima and minima, with the sign of the correlation depending strongly on whether pupil-linked arousal was high or low. These results suggest that variability in internal state modulates how the brain responds to external rhythmic stimulation and that arousal is a key factor coordinating the oscillatory mechanisms of the brain.

Facilitatory effect of arousal on low-frequency entrainment

A key finding in our study was that increases in the pupil size coincided with a selective increase of low-frequency phase entrainment to the task-relevant stimulus sequence. While previous work on arousal-related effects on cortical function has largely focused on processing of single stimuli (either unpredictable or predictable), how arousal may benefit the processing of rhythmic stimulation has been less studied. Previous research has found that diminished phase entrainment is associated with lapses in attention and response accuracy (van den Brink et al., 2014; Lakatos et al., 2016). Our finding suggests that transient decreases in pupil-linked arousal may be one factor underlying these observations. Studies in animals suggest that pupil dilation is associated with changes in neuronal excitability and population activity (Reimer et al., 2014; Vinck et al., 2015; McGinley et al., 2015a), tuning the cortex into an active state (McGinley et al., 2015b). In addition, increased arousal is often associated with better task performance at low-to-intermediate arousal levels, while task performance decreases at very high levels of pupil-linked arousal, giving rise to an inverted-U relation between pupil-linked arousal and performance (van den Brink et al., 2016; Waschke et al., 2019; Beerendonk et al., 2023). Interestingly, Figure 4a shows decreased task-relevant ITC in the time windows with the largest baseline pupil size (bin 10). Our findings suggest that pupil-linked arousal, by shaping the brain's internal state, affects how the brain processes task-relevant rhythmic stimuli.

Arousal-related neuromodulatory systems have been suggested to play a role in selective attention by setting the level of responsivity (i.e., gain) and excitability of the regions processing single stimuli that are salient or task-relevant (Dahl et al., 2022). In light of our results, one can speculate that while a "phasic" recruitment of neuromodulatory nuclei facilitates the processing of single stimuli, the "tonic" mode may be used for entrainment to sustained stimuli at low frequencies. While future studies are warranted to directly elucidate how neuromodulatory activity affects activity at the neuronal level during rhythmic stimulation, our results pose the arousal-related neuromodulatory systems as a highly flexible tool that can be recruited under different situations.

Evidence for entrainment versus alpha processing modes

While larger pupil size was associated with a selective increase in low-frequency phase entrainment, larger alpha power was associated with an overall decrease in phase entrainment. These contrasting effects are surprising, given that alpha power and pupil size showed a strong positive relationship, a similar relationship with task performance (i.e., negative quadratic relationship with number of incorrect responses), as well as a clear temporal relationship (Fig. 5c): alpha power peaked before pupil maxima and reached a minimum before pupil minima—a similar pattern as in Montefusco-Siegmund et al. (2022). Moreover, both the pupil size and alpha desynchronization are thought to reflect activity of the noradrenergic system (Dahl et al., 2022). On the other hand, the partly dissociable effects of the pupil size (positively correlated with task-relevant phase entrainment; Fig. 4a) and posterior alpha power (negatively correlated with entrainment; Fig. 4c) seem consistent with previous work suggesting that spontaneous fluctuations in pupil size and alpha power jointly shape perception but modulate different aspects, i.e., perceptual sensitivity and perceptual bias, respectively (Waschke et al., 2019; Pilipenko and Samaha, 2024). Our study thus offers new evidence on a partial dissociation between these variables as mechanisms modulating attention to rhythmic stimulation.

A recent framework of oscillatory mechanisms proposes the existence of processing modes: an "entrainment mode," in which sensory brain oscillatory mechanisms are engaged in processing rhythmic stimuli, and an "alpha-dominated mode," in which the brain decouples from external stimulation (Zoefel and Van Rullen 2017). Our results support this framework in the sense that higher alpha power was related to decreases in entrainment to any (task-relevant and task-irrelevant) stimuli. While evidence for these modes was found in monkeys (Lakatos et al., 2016), here we found this effect also in humans. This is a novel result because it may reflect a general attentional mechanism comprising exogenous (i.e., led by task structure) and endogenous (led by internal state) processes. Furthermore, our results suggest that the shift between these modes is dependent on the level of arousal, as we discuss below.

Arousal-dependent relation between prestimulus alpha power and low-frequency entrainment

Our exploratory analyses of the temporal relation between prestimulus alpha power, ITC, and pupil maxima/minima shed some light on the differential effects of pupil-linked arousal and alpha power: alpha power and task-relevant ITC showed a significant cross-correlation in the time windows around pupil maxima and minima, with the sign of the correlation depending strongly on whether pupil-linked arousal was high or low. We can only speculate why the coupling between entrainment and alpha power differed at the opposite extremes of arousal. One possibility is that the peaking of alpha power and correlation with ITC around pupil maxima reflected activity in brainstem arousal centers, which also drove the peaking of the pupil size. Indeed, activity in the locus ceruleus occurs shortly before pupil dilation (Joshi et al., 2016); pupil-linked arousal has generalized effects on the brain that are evident at slower time scales (Shine et al., 2016). On the other hand, the counter-relation around pupil minima may have reflected an inattention mechanism

within the alpha band that emerged at low arousal. Indeed, it has been proposed that top–down and primary sensory circuits may contribute to the alpha band with opposing effects (Bollimunta et al., 2008). During low arousal, cortical effects on alpha power may signal basic sensory processes, which are dissociated from pupil-linked arousal effects (Pilipenko and Samaha, 2024). Lakatos et al. (2016) reported a slow anticorrelation in nonhuman primates between alpha power and ITC, as discussed above, and a recent study in humans reported a similar anticorrelation with entrainment to auditory stimuli (Kasten et al., 2024). Intracranial measurements in humans also showed a modulation of alpha power by the phase of delta entrainment (Gomez-Ramirez et al., 2011). In terms of mechanisms of selective attention, we speculate that arousal is related to higher entrainment and cognitive contributions to alpha power (Sadaghiani and Kleinschmidt, 2016; Clayton et al., 2018). A slow countermodulation between sensory alpha power and entrainment, rather than being sustained, may emerge during periods of low arousal. Given that the results in humans and nonhuman primates suggest the translational value of the findings discussed here, future research should replicate and further disentangle the relation between alpha power and ITC during periods of high and low pupil-linked arousal.

Limitations and future directions

From a methodological perspective, it is hard to distinguish between true entrainment of ongoing neural oscillations and the consistent phase alignment caused by a sequence of stimulus-evoked potentials (Haegens and Golumbic 2018; van Diepen and Mazaheri, 2018; Helfrich et al., 2019). Nevertheless, mounting evidence shows that phase coherence persists during no-stimulus periods, suggesting that it is at least in part caused by neural entrainment (Zoefel et al., 2018; Bouwer et al., 2023), and intracranial studies in humans support the presence of widespread alignment of oscillations to rhythmic stimuli, not restricted to sensory areas (Besle et al., 2011; Gomez-Ramirez et al., 2011).

Previous studies have found within-trial phase–amplitude coupling between the delta phase of entrained oscillatory activity and alpha power over posterior brain regions (Wostmann et al., 2016; Wilson and Foxe, 2020). Here we were interested in fluctuations at slow time scales, similar to Lakatos et al. (2016), because they likely represent variation in the brain's internal states. To compute the uniformity of phase angles across stimulus sequences, we used 8 s sliding time windows. The length of these time windows did not allow for subsecond temporal resolution, limiting our ability to study stimuli-specific relationships between entrainment and alpha power at various levels of arousal. Taken together, our results and previous studies suggest that internally and externally driven oscillatory mechanisms operate at different time scales.

As our study design was based on Lakatos et al. (2016), we did not strictly counterbalance the order of the attend auditory and attend visual blocks or the presentation frequencies of the auditory and visual stimulus sequences (i.e., resulting in more auditory trials for the computation of ITC). We could afford this because none of our key hypotheses (i.e., those corresponding to Fig. 4) involved a direct comparison between the two perceptual modalities; instead, we recoded the stimulus sequences as "task-relevant" and "task-irrelevant" and focused our analyses on that distinction, as in Lakatos et al. (2016). Although the difference in presentation frequency may have driven the modality effects in ITC, it is interesting that none of the relationships we observed between ITC, alpha power, pupil size, and behavior showed systematic differences between the auditory and visual modalities. This supports the assumption that our results reflect fluctuations in internal state rather than modality-specific effects.

Future work could assess the relationship between phase entrainment and another internal state variable: the slope of the 1/f shape of the power spectrum—i.e., the aperiodic (nonoscillatory) component of EEG activity (Waschke et al., 2021). This slope has been proposed to track the ratio between excitation and inhibition in underlying neural circuitry (Gao et al., 2017) and has been found to covary with spontaneous fluctuations in pupil-linked arousal (Pfeffer et al., 2022). In addition, alpha power estimates may be more reliable if aperiodic EEG is taken into account (Cunningham et al., 2023).

Conclusions

Neural entrainment is an important instrument of selective attention (Schroeder and Lakatos, 2009). Here we reported delta-phase entrainment to both the visual and the auditory stimulus sequences, with stronger entrainment to the task-relevant modality than to the task-irrelevant modality. This is consistent with previous studies using bimodal stimulation (Besle et al., 2011; Lakatos et al., 2016). Most importantly, we found a significant linear relationship between pupil size and the degree to which entrainment tracked the task-relevant instead of the task-irrelevant stimulus sequence, indicating a facilitating effect of arousal on the perception of rhythmic stimulus sequences. We also found a coupling between alpha power and entrainment around pupil peaks and pupil troughs. Our results give clear indications of a differential modulation of brain oscillatory processes by arousal.

References

Bauer AKR, Van Ede F, Quinn AJ, Nobre AC (2021) Rhythmic modulation of visual perception by continuous rhythmic auditory stimulation. J Neurosci 41:7065–7075.

Beerendonk L, Mejías JF, Nuiten SA, de Gee JW, Fahrenfort JJ, van Gaal S (2023) A disinhibitory circuit mechanism explains a general principle of peak performance during mid-level arousal. bioRxiv 2023.07.28.550956.

Benedek M, Schickel RJ, Jauk E, Fink A, Neubauer AC (2014) Alpha power increases in right parietal cortex reflects focused internal attention. Neuropsychologia 56:393–400.

Besle J, Schevon CA, Mehta AD, Lakatos P, Goodman RR, McKhann GM, Emerson RG, Schroeder CE (2011) Tuning of the human neocortex to the temporal dynamics of attended events. J Neurosci 31:3176–3185.

Bollimunta A, Chen Y, Schroeder CE, Ding M (2008) Neuronal mechanisms of cortical alpha oscillations in awake-behaving macaques. J Neurosci 28:9976–9988.

Bouwer FL, Fahrenfort JJ, Millard SK, Kloosterman NA, Slagter HA (2023) A silent disco: differential effects of beat-based and pattern-based temporal expectations on persistent entrainment of low-frequency neural oscillations. J Cogn Neurosci 35:990–1020.

Bradshaw J (1967) Pupil size as a measure of arousal during information processing. Nature 216:515–516.

Ceh SM, Annerer-Walcher S, Körner C, Rominger C, Kober SE, Fink A, Benedek M (2020) Neurophysiological indicators of internal attention: an electroencephalography-eye-tracking coregistration study. Brain Behav 10:e01790.

Clayton MS, Yeung N, Cohen Kadosh R (2018) The many characters of visual alpha oscillations. Eur J Neurosci 48:2498–2508.

Cohen MX (2019) A better way to define and describe Morlet wavelets for time-frequency analysis. Neuroimage 199:81–86.

Compton RJ, Gearinger D, Wild H (2019) The wandering mind oscillates: EEG alpha power is enhanced during moments of mind-wandering. Cogn Affect Behav Neurosci 19:1184–1191.

Cooper NR, Croft RJ, Dominey SJ, Burgess AP, Gruzelier JH (2003) Paradox lost? Exploring the role of alpha oscillations during externally vs. internally directed attention and the implications for idling and inhibition hypotheses. Int J Psychophysiol 47:65–74.

Cunningham E, Zimnicki C, Beck DM (2023) The influence of prestimulus 1/f-like versus alpha-band activity on subjective awareness of auditory and visual stimuli. J Neurosci 43:6447–6459.

Dahl MJ, Mather M, Werkle-Bergner M (2022) Noradrenergic modulation of rhythmic neural activity shapes selective attention. Trends Cogn Sci 26:38–52.

Dal Ben R (2023) SHINE_color: controlling low-level properties of colorful images. MethodX 11:102377.

Delorme A, Makeig S (2004) EEGLAB: an open source toolbox for analysis of single-trial EEG dynamics including independent component analysis. J Neurosci Methods 134:9–21.

Ergenoglu T, Demiralp T, Bayraktaroglu Z, Ergen M, Beydagi H, Uresin Y (2004) Alpha rhythm of the EEG modulates visual detection performance in humans. Cogn Brain Res 20:376–383.

Gao R, Peterson EJ, Voytek B (2017) Inferring synaptic excitation/inhibition balance from field potentials. Neuroimage 158:70–78.

Gomez-Ramirez M, Kelly SP, Molholm S, Sehatpour P, Schwartz TH, Foxe JJ (2011) Oscillatory sensory selection mechanisms during intersensory attention to rhythmic auditory and visual inputs: a human electrocorticographic investigation. J Neurosci 31:18556–18567.

Groot JM, Boayue NM, Csifsák G, Boekel W, Huster R, Forstmann BU, Mittner M (2021) Probing the neural signature of mind wandering with simultaneous fMRI-EEG and pupillometry. Neuroimage 224:117412.

Haegens S, Golumbic EZ (2018) Rhythmic facilitation of sensory processing: a critical review. Neurosci Biobehav Rev 86:150–165.

Helfrich RF, Breska A, Knight RT (2019) Neural entrainment and network resonance in support of top-down guided attention. Curr Opin Psychol 29:82–89.

Henry MJ, Obleser J (2012) Frequency modulation entrains slow neural oscillations and optimizes human listening behavior. Proc Natl Acad Sci U S A 109:20095–20100.

Hong L, Walz JM, Sajda P (2014) Your eyes give you away: prestimulus changes in pupil diameter correlate with poststimulus task-related EEG dynamics. PLoS One 9:e91321.

Hopstaken JF, van der Linden D, Bakker AB, Kompier MA (2015) A multifaceted investigation of the link between mental fatigue and task disengagement. Psychophysiology 52:305–315.

Jin CY, Borst JP, van Vugt MK (2019) Predicting task-general mind-wandering with EEG. Cogn Affect Behav Neurosci 19:1059–1073.

Joshi S, Li Y, Kalwani RM, Gold JI (2016) Relationships between pupil diameter and neuronal activity in the locus coeruleus, colliculi, and cingulate cortex. Neuron 89:221–234.

Kasten FH, Busson Q, Zoefel B (2024) Opposing neural processing modes alternate rhythmically during sustained auditory attention. Commun Biol 7:1125.

Klimesch W, Sauseng P, Hanslmayr S (2007) EEG alpha oscillations: the inhibition-timing hypothesis. Brain Res Rev 53:63–88.

Kret ME, Sjak-Shie EE (2019) Preprocessing pupil size data: guidelines and code. Behav Res Methods 51:1336–1342.

Lakatos P, Barczak A, Neymotin SA, McGinnis T, Ross D, Javitt DC, O'Connell MN (2016) Global dynamics of selective attention and its lapses in primary auditory cortex. Nat Neurosci 19:1707–1717.

Lakatos P, Gross J, Thut G (2019) A new unifying account of the roles of neuronal entrainment. Curr Biol 29:R890–R905.

Lakatos P, Karmos G, Mehta AD, Ulbert I, Schroeder CE (2008) Entrainment of neuronal oscillations as a mechanism of attentional selection. Science 320:110–113.

Lakatos P, Schroeder CE, Leitman DI, Javitt DC (2013) Predictive suppression of cortical excitability and its deficit in schizophrenia. J Neurosci 33:11692–11702.

Madore KP, Khazenzon AM, Backes CW, Jiang J, Uncapher MR, Norcia AM, Wagner AD (2020) Memory failure predicted by attention lapsing and media multitasking. Nature 587:87–91.

Manzotti R (2017) A perception-based model of complementary afterimages. Sage Open 7:2158244016682478.

Martínez-Cancino R, Delorme A, Truong D, Artoni F, Kreutz-Delgado K, Sivagnanam S, Yoshimoto K, Majumdar A, Makeig S (2021) The open EEGLAB portal interface: high-performance computing with EEGLAB. Neuroimage 224:116778.

Mathewson KE, et al. (2012) Making waves in the stream of consciousness: entraining oscillations in EEG alpha and fluctuations in visual awareness with rhythmic visual stimulation. J Cogn Neurosci 24:2321–2333.

McGinley MJ, David SV, McCormick DA (2015a) Cortical membrane potential signature of optimal states for sensory signal detection. Neuron 87:179–192.

McGinley MJ, Vinck M, Reimer J, Batista-Brito R, Zagha E, Cadwell CR, Tolias AS, Cardin JA, McCormick DA (2015b) Waking state: rapid variations modulate neural and behavioral responses. Neuron 87:1143–1161.

Montefusco-Siegmund R, Schwalm M, Jubal R, Devia E, Egaña C, Maldonado JI, E P (2022) Alpha EEG activity and pupil diameter coupling during inactive wakefulness in humans. eNeuro 9: ENEURO.0060-21.2022.

O'Connell RG, Dockree PM, Robertson IH, Bellgrove MA, Foxe JJ, Kelly SP (2009) Uncovering the neural signature of lapsing attention: electrophysiological signals predict errors up to 20s before they occur. J Neurosci 29:8604–8611.

Pfeffer T, Keitel C, Kluger DS, Keitel A, Russmann A, Thut G, Donner TH, Gross J (2022) Coupling of pupil- and neuronal population dynamics reveals diverse influences of arousal on cortical processing. Elife 11:e71890.

Pilipenko A, Samaha J (2024) Double dissociation of spontaneous alpha-band activity and pupil-linked arousal on additive and multiplicative perceptual gain. J Neurosci 44:e1944232024.

Podvalny E, King LE, He BJ (2021) Spectral signature and behavioral consequence of spontaneous shifts of pupil-linked arousal in human. Elife 10:e68265.

Reimer J, Froudarakis E, Cadwell CR, Yatsenko D, Denfield GH, Tolias AS (2014) Pupil fluctuations track fast switching of cortical states during quiet wakefulness. Neuron 84:355–362.

Romei V, et al. (2008) Spontaneous fluctuations in posterior α-band EEG activity reflect variability in excitability of human visual areas. Cereb Cortex 18:2010–2018.

Sadaghiani S, Kleinschmidt A (2016) Brain networks and α-oscillations: structural and functional foundations of cognitive control. Trends Cogn Sci 20:805–817.

Samaha J, Gosseries O, Postle BR (2017) Distinct oscillatory frequencies underlie excitability of human occipital and parietal cortex. J Neurosci 37:2824–2833.

Schroeder CE, Lakatos P (2009) Low-frequency neuronal oscillations as instruments of sensory selection. Trends Neurosci 32:9–18.

Shine JM, Bissett PG, Bell PT, Koyejo O, Balsters JH, Gorgolewski KJ, Poldrack RA (2016) The dynamics of functional brain networks: integrated network states during cognitive task performance. Neuron 92:544–554.

Sivagnanam S, Majumdar A, Yoshimoto K, Astakhov V, Bandrowski A, Martone ME, Carnevale NT (2013) Introducing the Neuroscience Gateway, IWSG, volume 993 of CEUR Workshop Proceedings, CEUR-WS.org

Stefanics G, Hangya B, Hernádi I, Winkler I, Lakatos P, Ulbert I (2010) Phase entrainment of human delta oscillations can mediate the effects of expectation on reaction speed. J Neurosci 30:13578–13585.

Tallon-Baudry C, Bertrand O, Delpuech C, Pernier J (1996) Stimulus specificity of phase-locked and non-phase-locked 40 Hz visual responses in human. J Neurosci 16:4240–4249.

Ten Oever S, et al. (2017) Low-frequency cortical oscillations entrain to subthreshold rhythmic auditory stimuli. J Neurosci 37:4903–4912.

Unsworth N, Robison MK (2016) Pupillary correlates of lapses of sustained attention. Cogn Affect Behav Neurosci 16:601–615.

Unsworth N, Robison MK (2017) The importance of arousal for variation in working memory capacity and attention control: a latent variable pupillometry study. J Exp Psychol Learn Mem Cogn 43:1962.

van den Brink RL, Murphy PR, Nieuwenhuis S (2016) Pupil diameter tracks lapses of attention. PLoS One 11:e0165274.

van den Brink RL, Wynn S, Nieuwenhuis S (2014) Post-error slowing as a consequence of disturbed low-frequency oscillatory phase entrainment. J Neurosci 34:11096–11105.

van Diepen RM, Mazaheri A (2018) The caveats of observing inter-trial phase-coherence in cognitive neuroscience. Sci Rep 8:2990.

van Kempen J, Loughnane GM, Newman DP, Kelly SP, Thiele A, O'Connell RG, Bellgrove MA (2019) Behavioural and neural signatures of perceptual decision-making are modulated by pupil-linked arousal. Elife 8:e42541.

VanRullen R, et al. (2014) On the cyclic nature of perception in vision versus audition. Philos Trans R Soc B Biol Sci 369:20130214.

Vinck M, Batista-Brito R, Knoblich U, Cardin JA (2015) Arousal and locomotion make distinct contributions to cortical activity patterns and visual encoding. Neuron 86:740–754.

Waschke L, Donoghue T, Fiedler L, Smith S, Garrett DD, Voytek B, Obleser J (2021) Modality-specific tracking of attention and sensory statistics in the human electrophysiological spectral exponent. Elife 10:e70068.

Waschke L, Tune S, Obleser J (2019) Local cortical desynchronization and pupil-linked arousal differentially shape brain states for optimal sensory performance. Elife 8:e51501.

Wilson TJ, Foxe JJ (2020) Cross-frequency coupling of alpha oscillatory power to the entrainment rhythm of a spatially attended input stream. Cogn Neurosci 11:71–91.

Wöstmann M, Herrmann B, Maess B, Obleser J (2016) Spatiotemporal dynamics of auditory attention synchronize with speech. Proc Natl Acad Sci U S A 113:3873–3878.

Zoefel B, Ten Oever S, Sack AT (2018) The involvement of endogenous neural oscillations in the processing of rhythmic input: more than a regular repetition of evoked neural responses. Front Neurosci 12:95.

Zoefel B, VanRullen R. (2017). Oscillatory mechanisms of stimulus processing and selection in the visual and auditory systems: state-of-the-art, speculations and suggestions. Front Neurosci 11:296.